habitat islands, and to what are called habitat patches, or fragments, in the metapopulation literature (*7*).

11. Without any loss of generality, we assume that m_w equals unity.
12. M. E. Gilpin and J. M. Diamond, *Proc. Natl. Acad. Sci. U.S.A.* **73**, 4130 (1976); I. Hanski, *Trends Ecol. Evol.* **9**, 131 (1994); *J. Anim. Ecol.* **63**, 151 (1994). In the latter two references, the more general relation $\mu_{ij} = e/K_{ij}^{x}$ is used, but we assume here for simplicity that $x = 1$, which is a good approximation for many species. The rate parameter e has been here absorbed in the unit of island area, to give the per-year extinction probability $1 - e^{-1/A}$ for species with $w = 1$. A scaling constant d is given by $d = A'/A$, where A' is island area in (say) kilometers squared. d may be calculated from knowledge of the per-year extinction probability and A'.
13. T. W. Schoener, in *16th International Ornithological Congress*, Canberra, Australia, 12 to 17 August 1974 (Australian Academy of Sciences, Canberra City, 1976), pp. 629–642.
14. Somewhat confusingly, the classical metapopulation scenario, where there is no external mainland, is referred to as the "mainland" regression in the species-area literature.
15. The equilibrium probability of species i occupying island j, p_{ij}^*, which is called the incidence, J_{ij}, is obtained from Eq. 1 as

$$p_{ij}^* = J_{ij} = \frac{C_i^* w_i A_j}{C_i^* w_i A_j + 1} \quad (2)$$

where C_i^* is the equilibrium value of $C_i(t)$. In the mainland-island model, where $C_i(t) = cw_i$, we obtain

$$J_{ij} = \frac{cA_j w_i^2}{cA_j w_i^2 + 1} \quad (3)$$

In the metapopulation model, the incidences can be calculated only numerically. Substituting Eq. 2 into the expression $C_i^* = cw_i \Sigma J_{ij} A_j$, which gives the equilibrium value of $C_i(t)$ in the metapopulation model, we obtain

$$1 = cw_i^2 \sum_{j=1}^{R} \frac{A_j^2}{C_i^* w_i A_j + 1} \quad (4)$$

from which C_i^* can be solved provided that $cw_i^2 \Sigma A_j^2 > 1$, which is a necessary and sufficient condition for species i to persist in the network of islands. The incidences can then be calculated from Eq. 2.

16. O. Arrhenius, *J. Ecol.* **9**, 95 (1921); H. A. Gleason, *Ecology* **3**, 158 (1922); F. W. Preston, *ibid.* **41**, 611 (1960).
17. M. H. Buys, J. S. Maritz, J. J. A. Van Der Walt, *J. Veg. Sci.* **5**, 63 (1994); M. R. Williams, *Ecology* **76**, 2607 (1995).
18. The nonlinear logistic model can be linearized with the logit-transformation, $\log [P/(1 - P)] = a + b \log w$, which we apply throughout this report.
19. Assuming that Q (species number in the pool) is large and that $\log w$ is uniformly distributed with zero mean, we obtain after some calculation the expected number of species on island j as

$$S_j = \Sigma_i J_{ij} = \frac{Q}{4\sigma_w \sqrt{3}} \log \Gamma \quad (5)$$

where (dropping the subscript j)

$$\Gamma = \frac{1 + cA\, e^{2\sigma_w \sqrt{3}}}{1 + cA\, e^{-2\sigma_w \sqrt{3}}}$$

The slope of the SA curve is then given by

$$\frac{\partial \log S}{\partial \log A} = \frac{1 - \Gamma^{-1}}{\Gamma \log \Gamma} \quad (6)$$

The distribution of species i is given by

$$P_i = \frac{1}{R} \Sigma_j J_{ij} = 1 - \frac{1}{2\sigma_A \sqrt{3}} \log \frac{cw_i^2 + q_1}{cw_i^2 + q_2} \quad (7)$$

and the slope of the DA curve is (dropping the subscripts)

$$\frac{\partial \log (P/[1 - P])}{\partial \log w} = \frac{2\, cw^2 q}{(cw^2 + q_1)(cw^2 + q_2) P(1 - P)} \quad (8)$$

where

$$q_1 = e^{-m_A + \sigma_A \sqrt{3}},\ q_2 = e^{-m_A - \sigma_A \sqrt{3}},$$

$$\text{and } q = \frac{1}{2\sigma_A \sqrt{3}} [q_1 - q_2]$$

20. σ_w can be estimated as the standard deviation of the species abundance distribution on the mainland. In 10 examples of invertebrate and bird communities, empirical values ranged from 0.95 to 2.57 (mean = 1.63, SD = 0.62; details can be obtained from I.H. upon request). G. Sugihara [*Am. Nat.* **116**, 770 (1980)] has reported a wider range of values than reported here, but the data in his study do not always represent "local" communities (for example, birds in North America). Using Eq. 3, one can express the parameter combination cA as $cA = w^{-2} J/(1 - J)$, which suggests that, in principle, c can be estimated with data on island areas, species' abundances on mainland, and on their incidences on islands. To aid intuition about the cA values, consider an average species with $w_i = 1$. For such a species, $cA = J/(1 - J)$, and hence the range of cA values in Fig. 3A from 10^{-2} to 10^{2} corresponds to the incidence on average-sized islands ranging from 0.01 to 0.99, which covers a very large range.
21. Denoting the per-year colonization and extinction probabilities by λ and μ, we obtain

$$cA = \frac{\lambda}{\mu} E[w^2]$$

where E denotes the expected value. That the slope of the SA curve depends on the ratio of colonization to extinction probabilities has been suggested by R. E. Ricklefs and G. W. Cox [*Am. Nat.* **106**, 195 (1972)] and M. P. Johnson and D. S. Simberloff [*J. Biogeogr.* **1**, 149 (1974)].
22. The vertical asymptote in Fig. 1H is given by

$$\log w = -\frac{1}{2}\left(\log c + \log \sum_{j=1}^{R} A_j^2\right)$$

The other asymptote has a slope of 2.

23. We derived the slope values (*19*) also for back-to-back exponential and lognormal distributions of w. The expressions are more complicated in these cases, but the results are very similar.
24. F. W. Preston, *Ecology* **43**, 185 (1962); R. M. May, in *Ecology and Evolution of Communities*, M. L. Cody and J. M. Diamond, Eds. (Belknap, Cambridge, MA, 1975), p. 81.
25. C. Wissel and B. Maier, *J. Biogeogr.* **19**, 355 (1992).
26. B. D. Coleman, *Math. Biosci.* **54**, 191 (1981); H. Caswell and J. E. Cohen, in *Species Diversity in Ecological Communities: Historical and Geographical Perspectives*, R. E. Ricklefs and D. Schluter, Eds. (Univ. of Chicago Press, Chicago, 1993), p. 99.
27. B. D. Patterson, *Conserv. Biol.* **1**, 323 (1987).
28. M. Nieminen, *Oecologia* **108**, 643 (1996). The moth example includes 46 islands located about 15 km off the mainland in southwest Finland. Moths were trapped with sugar-bait traps in summer 1993. The parameter $\log w$ gives the abundance on mainland.
29. Z. Witkowski and P. Płonka, *Bull. Pol. Acad. Sci. Biol. Sci.* **32**, 241 (1984); W. B. Harms and P. Opdam, in *Changing Landscapes: An Ecological Perspective*, I. G. Zonneveld and R. T. T. Forman, Eds. (Springer-Verlag, New York, 1990), p. 73. The bird examples are from studies in Poland (Witkowski and Płonka) and The Netherlands (Harms and Opdam). "Islands" in this instance are habitat islands on mainland. The parameter $\log w$ in Fig. 1H gives the estimated density of territories.
30. E. F. Connor and E. C. McCoy, *Am. Nat.* **113**, 791 (1979).
31. We thank F. Adler, J. Brown, M. Camara, E. Connor, M. Kuussaari, J. Lawton, A. Moilanen, and T. Schoener for comments on the manuscript. W. W. Murdoch and National Center for Ecological Analysis and Synthesis (NCEAS) in Santa Barbara are thanked for supporting this research.

30 September 1996; accepted 27 November 1996

Reduced Ubiquitin-Dependent Degradation of c-Jun After Phosphorylation by MAP Kinases

Anna Maria Musti,* Mathias Treier,† Dirk Bohmann‡

The proto-oncogene–encoded transcription factor c-Jun activates genes in response to a number of inducers that act through mitogen-activated protein kinase (MAPK) signal transduction pathways. The activation of c-Jun after phosphorylation by MAPK is accompanied by a reduction in c-Jun ubiquitination and consequent stabilization of the protein. These results illustrate the relevance of regulated protein degradation in the signal-dependent control of gene expression.

The ubiquitin-dependent protein degradation system is used in the cell not just to eliminate proteins that are either damaged or no longer needed. Instead, it fulfills important functions in cell regulation and signal transduction such as the cell cycle–specific degradation of cyclins and the cytokine-induced breakdown of the transcription factor inhibitor IkB (*1–5*).

The transcription factor c-Jun is an in vivo substrate for multi-ubiquitination (*6*). We investigated whether the ubiquitin-dependent breakdown of c-Jun is a constitutive process or is regulated and whether it might contribute to signal transduction through c-Jun.

One mechanism by which intracellular information is transduced to c-Jun is the phosphorylation of the protein by MAPK-type enzymes, such as the JNKs and the ERKs

European Molecular Biology Laboratory, Meyerhofstr. 1, 69117 Heidelberg, Germany.

*On leave from Centro Endocrinologia ed Oncologia Sperimentale, CNR, Naples, Italy.
†Present address: Howard Hughes Medical Institute, University of California, San Diego, La Jolla, CA 92093–0648, USA.
‡To whom correspondence should be addressed.

(*7–9*). Phosphorylation of c-Jun by MAPK on Ser^{63} and Ser^{73}, as well as on Thr^{91} or Thr^{93}, or both, increases its trans-activating potential and DNA-binding activity (*10–12*). The location of these sites in the vicinity of the δ domain, which mediates c-Jun multi-ubiquitination and degradation (*6*), raised the possibility of a functional connection between phosphorylation and ubiquitination. To investigate this idea, we examined the effect of phosphorylation on the ubiquitination of c-Jun in vivo. Histidine-tagged c-Jun was expressed with epitope-tagged ubiquitin in NIH 3T3 cells. This experimental design permits the purification and detection of multi-ubiquitinated forms of c-Jun, which can be visualized as ladders of immunoreactivity on a protein immunoblot (Fig. 1).

To examine a potential effect of c-Jun phosphorylation, we carried out the same experiment in the presence of vectors directing the expression of JNK1 (*13*) and an activator of JNK1, a gain-of-function mutant of the small guanine nucleotide–binding protein Cdc42 (*14*). Under these conditions, most of the histidine-tagged c-Jun became phosphorylated, as shown by the slower migration of the protein in the SDS-polyacrylamide gel (Fig. 1). Concomitant with the increase of phosphorylation, the multi-ubiquitination of c-Jun was reduced (Fig. 1). To exclude the possibility that increased JNK1 or Cdc42 activity has a general effect on the ubiquitination machinery in the transfected cells, we analyzed a mutant of c-Jun in which the MAPK phosphorylation sites were replaced by alanine residues ($c\text{-}Jun^{Ala}$). The ubiquitination of this nonphosphorylatable version of c-Jun was not decreased by cotransfection of JNK and Cdc42, indicating that the decrease in ubiquitination is a direct consequence of phosphorylation of c-Jun.

To investigate whether phosphorylation of the MAPK sites in c-Jun might be sufficient to decrease ubiquitination, we examined the ubiquitination of a mutant of c-Jun ($c\text{-}Jun^{Asp}$) in which the phosphorylation sites were replaced by phosphate-mimetic aspartic acid residues. This mutant, $c\text{-}Jun^{Asp}$, acts as a gain-of-function form of c-Jun (*11*, *15*). Indeed, $c\text{-}Jun^{Asp}$ was inefficiently multi-ubiquitinated, whereas the corresponding alanine-replacement mutant was ubiquitinated with at least the same efficiency as the wild-type protein (Fig. 2).

Phosphorylation by JNK not only suppressed multi-ubiquitination but also stabilized c-Jun in vivo (Fig. 3). Epitope-tagged wild-type c-Jun and the corresponding Jun^{Ala} and Jun^{Asp} mutants were transiently transfected in 3T3 cells and metabolically labeled with ^{35}S. The decay of c-Jun after the radioactivity was removed from the culture medium was consistent with the previously reported half-life of ~90 min. When phosphorylated by cotransfection of JNK, however, the half-life of phosphorylated c-Jun was two- to threefold longer than that of dephosphorylated c-Jun. Jun^{Ala} was refractory to JNK phosphorylation and consistently showed fast degradation kinetics regardless of whether or not it was cotransfected with the kinase. In contrast, Jun^{Asp}, even in the absence of JNK, had a half-life that was 3.5 times as long as that of the wild-type and Jun^{Ala} proteins. These results indicate that phosphorylation by JNK regulates the half-life of c-Jun.

The regulatory process described here likely contributes to the efficient activation of target genes after exposure of cells to

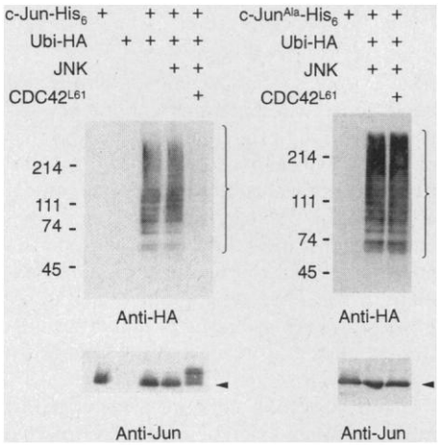

Fig. 1. Inhibition of c-Jun ubiquitination after phosphorylation by JNK. NIH 3T3 cells were transfected with expression vectors (1 μg) for c-Jun-His_6, $c\text{-}Jun^{Ala}$-His_6, ubiquitin-HA (Ubi-HA), and 2 μg of each expression plasmid containing cDNA for human JNK1 (JNK) and the activated form of Cdc42 ($Cdc42^{L61}$). His_6-tagged c-Jun–ubiquitin conjugates were purified from lysates and analyzed by SDS-PAGE (10% gel) and protein immunoblotting with a monoclonal antibody to HA (anti-HA) and a chemoluminescence detection system (upper panels) (*18*). The apparent molecular sizes (in kilodaltons) of protein standards are shown on the left. The position of c-Jun–ubiquitin conjugates is indicated on the right. The lower panels show the same blots analyzed with polyclonal antibody to Jun. The arrowhead indicates the position of dephosphorylated c-Jun. The phosphorylated Jun protein migrates more slowly. This immunoblot was developed with a phosphatase-conjugated second antibody; under these conditions only the majority of c-Jun (which is in the nonubiquitinated form) is visualized.

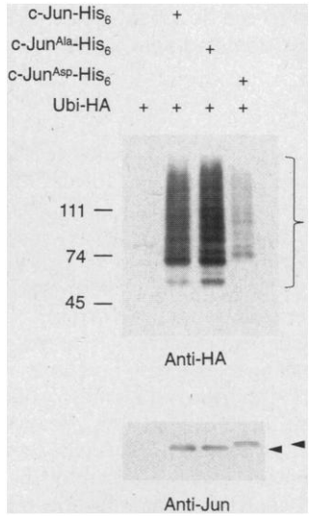

Fig. 2. In vivo ubiquitination of c-Jun substitution mutants $c\text{-}Jun^{Ala}$ and $c\text{-}Jun^{Asp}$. Expression vectors for hexahistidine (His_6)-tagged c-Jun (1 μg) or His_6-tagged c-Jun substitution mutants, $c\text{-}Jun^{Ala}$-His_6 and $c\text{-}Jun^{Asp}$-His_6, were transfected into Hela TK^- cells along with vectors for HA-tagged ubiquitin (1 μg) as indicated (*19*). Ubiquitin-conjugates of His_6-tagged c-Jun were purified by nickel-chelate affinity chromatography and analyzed by SDS-PAGE (10% gel) and protein immunoblotting with anti-HA (upper panel) (*19*). The molecular sizes of protein standards (in kilodaltons) are shown on the left. The position of conjugates of His_6-tagged c-Jun proteins and HA-tagged ubiquitin is indicated on the right. The lower panel shows the same blot developed with a polyclonal antibody raised in rabbits against bacterially expressed full-length c-Jun. The arrowhead indicates the position of the various His_6-tagged c-Jun proteins. The lower electrophoretic mobility of the $c\text{-}Jun^{Asp}$ mutant reflects the "pseudo-phosphorylated" properties of the protein (*11*).

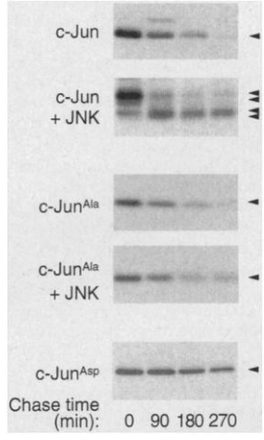

Fig. 3. Stabilization of c-Jun by phosphorylation. The stability of HA-tagged c-Jun and Jun^{Ala} before and after phosphorylation and of Jun^{Asp} was compared by measuring the decay of radiolabeled proteins (arrowheads) in 3T3 cells (*20*). c-Jun phosphorylation was induced by cotransfection of JNK1 and anisomycin treatment during and after labeling and is apparent by the additional slower migrating bands (multiple arrowheads). The top two panels show that the half-life of phosphorylated c-Jun is longer than that of dephosphorylated c-Jun (two- to threefold, as determined by phosphoimaging analysis). The stability of nonphosphorylatable Jun^{Ala} is not affected by JNK (middle panels) and is similar to that of dephosphorylated c-Jun. $c\text{-}Jun^{Asp}$ shows increased stability even without JNK induction (bottom panel).

growth factors, stress, or other inducers of c-Jun activity. Such an effect might be compounded by a similar regulation of the Jun partner molecule, c-Fos, which also exhibits phosphorylation-dependent changes of its half-life (*16*).

REFERENCES AND NOTES

1. V. J. Palombella, O. J. Rando, A. L. Goldberg, T. Maniatis, *Cell* **78**, 773 (1994).
2. M. Glotzer, A. M. Murray, M. W. Kirschner, *Nature* **349**, 132 (1991).
3. A. Isaksson, A. M. Musti, D. Bohmann, *Biochim. Biophys. Acta* **1288**, 21 (1996).
4. S. Jentsch and S. Schlenker, *Cell* **82**, 881 (1995).
5. M. Hochstrasser, *Curr. Opin. Cell Biol.* **7**, 215 (1995).
6. M. Treier, L. M. Staszewski, D. Bohmann, *Cell* **78**, 787 (1994).
7. R. Treisman, *Curr. Opin. Cell Biol.* **8**, 205 (1996).
8. M. Treier and D. Bohmann, in *Protein Phosphorylation*, F. Marks, Ed. (Verlag Chemie, Weinheim, 1996), pp. 297–327.
9. F. A. Peverali *et al.*, *EMBO. J.* **15**, 3943 (1996).
10. B. Binetruy, T. Smeal, M. Karin, *Nature* **351**, 122 (1991).
11. A. G. Papavassiliou, M. Treier, D. Bohmann, *EMBO J.* **14**, 2014 (1995).
12. B. J. Pulverer, J. M. Kyriakis, J. Aruch, E. Nikolakaki, J. R. Woodgett, *Nature* **353**, 670 (1991).
13. B. Dérijard *et al.*, *Cell* **76**, 1025 (1994).
14. O. A. Coso *et al.*, *ibid.* **81**, 1137 (1995).
15. M. Treier, D. Bohmann, M. Mlodzik, *ibid.* **83**, 753 (1995).
16. K. Okazaki and N. Sagata, *EMBO J.* **14**, 5048 (1995).
17. F. L. Graham and A. J. van der Eb, *Virology* **52**, 456 (1973).
18. JNK1 and Cdc42^{L61} expression vectors have been described (*14*). NIH 3T3 cells were transiently transfected by calcium phosphate coprecipitation (*17*). Purification of c-Jun–ubiquitin conjugates and protein immunoblot analysis were done as described (*6*). Ubiquitination assays were performed in HeLa or in NIH 3T3 cells with either His_6-tagged or HA-tagged c-Jun expression vectors with essentially identical results (compare Figs. 1 and 2).
19. His_6-tagged c-Jun expression vectors have been described (*6*). c-Jun^{Ala}-His_6 and c-Jun^{Asp}-His_6 eukaryotic expression vectors were generated as described for His_6-tagged wild-type c-Jun (*11*). The c-Jun^{Ala} mutant contains alanine residues in place of serines or threonines at position 58, 62, 63, 73, 89, 90, 91, 93, and 95; c-Jun^{Asp} contains aspartic acid residues in place of the serines and threonines at position 58, 62, 63, 73, 91, and 93. The hemagglutinin (HA)-tagged ubiquitin eukaryotic expression vector, Hela thymidine kinase–negative (TK$^-$) cell transfections, purification of Jun-ubiquitin conjugates, and immunoblot analysis were as described (*6*).
20. The cytomegalovirus-based expression vectors for HA-tagged c-Jun and JNK1 have been described (*6*, *14*). The c-Jun substitution mutants were generated as described (*11*). NIH 3T3 cells were transfected by calcium phosphate precipitation (*17*) with 0.25 μg of the respective c-Jun expression vector and 3 μg of JNK expression vector as indicated. After 24 hours, cells were radioactively labeled for 30 min with 75 mCi of ^{35}S-methionine and ^{35}S-cysteine per milliliter of medium, followed by incubation in a medium that contained 2 mM each of unlabeled methionine and cysteine for 0, 90, 180, or 270 min. The cells that had been transfected with the JNK1 expression vector were treated with 10 mM anisomycin during the labeling and chase periods to induce kinase activity. Cells were lysed in RIPA buffer [10 mM tris (pH 7.5), 45 mM β-glycerophosphate, 50 mM NaF, 5 mM sodium molybdate, 0.1% SDS, 1 mM EDTA, 1% NP-40, 0.5% deoxycholate] supplemented with 1 mM phenylmethylsulfonyl fluoride and 10 mg each of leupeptin, aprotinin, and pepstatin per milliliter of buffer. Samples containing equal amounts of acid-insoluble radioactivity were incubated with protein G– and protein A– agarose (Oncogene Science) and then incubated with the monoclonal antibody 12CA5 to HA. Precipitates were collected on protein G– and protein A–agarose, washed once with buffer A [10 mM tris (pH 7.5), 45 mM β-glycerophosphate, 50 mM NaF, 5 mM sodium molybdate, 0.1% SDS, 1 mM EDTA, 0.5% NP-40], once with buffer B [10 mM tris (pH 7.5), 410 mM NaCl, 45 mM β-glycerophosphate, 0.1% SDS, 1 mM EDTA, 0.5% NP-40], once with 10 mM tris (pH 7.5), and analyzed by SDS–polyacrylamide gel electrophoresis (PAGE; 10% gel) and autoradiography.

21. We thank S. Gutkind for plasmid vectors, L. Staszewski for technical assistance, and I. Mattaj, S. Cohen, T. Graf, A. Isaksson, L. Kockel, A. Papavassilou, and C. Ovitt for comments on the manuscript. Supported by a grant from the CNR to A.M.M.

19 June 1996; accepted 28 October 1996

Transmission of the BSE Agent to Mice in the Absence of Detectable Abnormal Prion Protein

Corinne I. Lasmézas,* Jean-Philippe Deslys, Olivier Robain, Alexandre Jaegly, Vincent Beringue, Jean-Michel Peyrin, Jean-Guy Fournier, Jean-Jacques Hauw, Jean Rossier, Dominique Dormont

The agent responsible for transmissible spongiform encephalopathies (TSEs) is thought to be a malfolded, protease-resistant version (PrPres) of the normal cellular prion protein (PrP). The interspecies transmission of bovine spongiform encephalopathy (BSE) to mice was studied. Although all of the mice injected with homogenate from BSE-infected cattle brain exhibited neurological symptoms and neuronal death, more than 55 percent had no detectable PrPres. During serial passage, PrPres appeared after the agent became adapted to the new host. Thus, PrPres may be involved in species adaptation, but a further unidentified agent may actually transmit BSE.

One of the distinct features of the BSE agent is its high ability to infect other species (*1–3*), whereas other TSE agents are easily transmitted only within a species. This species barrier leads to considerable prolongation of the incubation period during interspecies transmission (*4*). During subsequent experimental passages, TSE agents adapt to the new host: the incubation period shortens and stable pathological properties are acquired (*5*). According to the prion hypothesis, PrPres (the pathological, protease-resistant isoform of the prion protein) constitutes the infectious agent in TSEs, and replication involves the homotypic interaction between a pathological PrP molecule and the endogenous native protein to produce a conformational conversion to the abnormal isoform. The magnitude of the species barrier would thus be a condition of the extent of congruency between the PrP of the donor species and that of the new host (*6*). However, this mechanism cannot account for the exceptional ability of the BSE agent to cross the species barrier. This agent has original properties and is suspected to have contaminated humans (*2*, *7*). Thus, we examined BSE transmission and PrPres during primary transmission to mice and in subsequent passages to other mice.

Thirty C57BL/6 mice were inoculated by intracerebral injection of a 25% BSE-infected cattle brain homogenate. After 368 to 719 days, all of the inoculated animals exhibited symptoms of a neurological disease encompassing mainly hindlimb paralysis, tremors, hypersensitivity to stimulation, apathy, and a hunched posture. Biochemical analysis of their brains showed no detectable PrPres accumulation in more than 55% of the mice; these mice were termed PrPres$^-$ (Figs. 1 and 2) (*8*). Histological examination revealed neuronal death in all mice, but other classical changes associated with TSEs—that is, neuronal vacuolation and astrocytosis—were limited to the PrPres$^+$ mice (Fig. 3). Neuronal loss was most obvious in the Purkinje cells of the cerebellum, but degenerated neurons were also observed, to a smaller extent, in the CA1 region of the hippocampus. No sign of local inflammation was present. Electron microscopic examination of degenerated cells

C. I. Lasmézas, J.-P. Deslys, A. Jaegly, V. Beringue, J.-M. Peyrin, D. Dormont, Commissariat à l'Energie Atomique, Service de Neurovirologie, DSV/DRM/SSA, B.P. 6, 60-68 avenue du General Leclerc, 92265 Fontenay-aux-Roses Cedex, France.
O. Robain, Hôpital Saint Vincent de Paul, INSERM U 29, 74 avenue Denfert-Rochereau, 75674 Paris Cedex 14, France.
J.-G. Fournier, Hôpital de la Salpétrière, INSERM U 153, 47 boulevard de l'Hôpital, 75651 Paris Cedex 13, France.
J.-J. Hauw, Hôpital de la Salpétrière, Laboratoire Escourolle, INSERM U 360, 47 boulevard de l'Hôpital, 75651 Paris Cedex 13, France.
J. Rossier, Ecole Supérieure de Physique et Chimie Industrielles, CNRS URA 2054, 10 rue Vauquelin, 75231 Paris Cedex 5, France.

*To whom correspondence should be addressed. E-mail: CORINNE.LASMEZAS@cea.fr